

Microemulsion Copolymerization Modeling Study Via a Combined Integral-Differential Experimental Data Processing Approach

F. López-Serrano,^{*1} E. Mendizábal,² J.E. Puig,² J. Álvarez³

Summary: On the basis of the data processing technique associated with the integro-differential (ID) modeling assessment methodology, the styrene-acrylonitrile microemulsion copolymerization system is studied, with a three-state (conversion, active particles and micelles) and four-parameter model (entrance and exit of radicals to and from particles, monomer transport from micelles to growing particles and initial micelle number), in conjunction with experimental conversion measurements. Comparing with the standard regression method, employed in previous studies, the ID approach incorporates additional information contained in the smooth conversion measurement derivative and does not require relying on a constant number of particles, as the slope-and-intercept method does. The resulting model, tested at three initiator concentrations, temperatures and comonomer feed, describes the S-shaped conversion and the bell-shaped active particles evolutions. This last finding is contrary to previous assumptions on linear growth with time of active particles. As expected, the entry and exit rate coefficients increase with initiator and styrene concentration and temperature. The surfactant transport from micelles decreases with initiator concentration and the initial micelles concentration value only affects the entry rate.

Keywords: acrylonitrile; copolymerization; integro-differential method; mathematical model; microemulsion; styrene

Introduction

Microemulsion (ME) polymerization is a process in which latex containing very small polymer particles (between 10–50 nm) of high molar masses ($> 10^6$ Da) are obtained at high reaction rates. Batch emulsion and microemulsion polymerization differ, among other things, in the intervals observed in the rate of polymerization. In the first case, three intervals are observed

and only two in microemulsion. Regarding the calculation of entry and exit rate coefficients, to and from polymerizing particles respectively, the so-called slope-and-intercept method has been proposed.^[1] The limitation of this method is that it is valid only in intervals II or III, but a constant number of particles is required; that is, a seeded polymerization. In the literature, few models for microemulsion copolymerization have been stated. Sanghvi et al.^[2] reported a simple model for microemulsion copolymerization with low-conversion prediction capability. Ovando-Medina et al.^[3] proposed a model that predicts the microemulsion copolymerization kinetics of styrene (STY) and butyl acrylate (BA) thorough the whole reaction; however, it is complicated, since several assumptions are involved and many

¹ Facultad de Química, Dpto. Ing. Quím., Universidad Nacional Autónoma de México. DF 04510. México Fax: (52) 55 5622 5361;

E-mail: lopezserrano@correo.unam.mx

² CUCEI, Universidad de Guadalajara. Guadalajara, Jalisco 44430. México

³ Departamento de Ingeniería de Procesos e Hidráulica, Universidad Autónoma Metropolitana-Iztapalapa, DF 09340. México

parameters are required. A simple mechanistic four-parameter copolymerization model is presented here as an extension to our model for ME homopolymerization,^[4,5] based on the integro-differential (ID) model assessment-parameter fitting approach,^[6,7] which exploits the model identification capability offered by its differential (D) method step supported by a nonlinear instantaneous observability property,^[8] in the understanding that this capability is not present in the parameter fitting approach with purely integral regression that has been employed in polymer kinetic modeling studies.^[9 and references therein]

The resulting copolymer model is tested with conversion data from Sanghvi et al.^[2] for the styrene (STY) – acrylonitrile (AN) copolymerization varying initiator concentration, temperature and the initial monomers mixture composition.

Modeling Problem

In the model, the following considerations are made: (i) a 0–1 compartmentalized (zero or one radical in polymer particles) system, (ii) monomer concentration in the particles decreases linearly with conversion,^[2,10] (iii) there is no coagulation between particles, (iv) monomer and emulsifier are fed from micelles to growing particles,^[4,5] (v) radicals from the aqueous phase enter micelles but not the particles,^[4,5,11] and (vi) exit of radicals from particles can occur after transfer reactions to monomer giving as a result dead particles (with zero radicals).

According to the previously reported monomer partition expression,^[2,10] the states evolution can be expressed as:

$$\begin{aligned}\dot{x} &= K(1-x)N_1(t), \\ K &= (k_p C_m)/(M_o N_{av}); \\ x(0) &= x_o, \quad y = x\end{aligned}\quad (1a)$$

$$\dot{N}_m = -\rho_m N_m - k_m N_m N_1; \quad (1b)$$

$$\begin{aligned}N_m(0) &= N_{m0} \\ \dot{N}_1 &= \rho_m N_m - k N_1; \quad N_1(0) = 0\end{aligned}\quad (1c)$$

where x is the conversion, and y is its experimental measurement, (\cdot) is the time derivative of (\cdot) , N_1 is the concentration of active particles (L^{-1}), k_p ($L \text{ mol}^{-1} \text{ s}^{-1}$) is the propagation rate constant, C_m ($\text{mol } L^{-1}$) is an experimentally measured parameter,^[2,10] M_o ($\text{mol } L^{-1}$) is the initial monomer concentration and N_{av} is the Avogadro's number. N_m (L^{-1}) is the micelles concentration and represents the micelles number evolution as described by López-Serrano et al.^[4,5] The first-order radical entry to micelles is ρ_m (s^{-1}) and the radicals desorption constant is k (s^{-1}). The second-order surfactant transport rate coefficient from micelles to particles is k_m ($L \text{ s}^{-1}$). Regarding this last term, if one were to treat the problem as modeled in mass transport, a concentration gradient and the mass transfer area should be included, increasing the difficulty of the problem and the unknown parameters. Actually, the second term in Eq 1b corresponds to an action mass law which implies that k_m is not a mass transport rate coefficient, but a kind of collision rate coefficient. Here, this approximation is performed as a first approach. The modeling assessment problem consists in estimating the four-parameter set N_{m0} – ρ_m – k – k_m on the basis of the conversion measurement $y(t)$ and the three-state dynamic model (1), in the understanding that the direct application of the standard regression-based integral approach is by no means a straightforward task because of the large ratio of adjustable parameters to experimental measurements.^[11 and references therein]

The Proposed Model

Following the differential step of the ID model assessment approach, the smoothed-filtered^[4–7] conversion data trend $y(t)$ and its derivative $y_{\cdot}(t)$ are obtained in analytic form, and equation (1a) is solved for the scaled value N_{1a} of the active particle evolution

$$\begin{aligned}N_{1a}(t) &= [y_{\cdot}(t)]/\{[1-y(t)]\}, \\ N_{1a} &= K N_{1e}\end{aligned}\quad (2)$$

in the understanding that: (i) in copolymerization it is more likely that k_p (contained in K) would be time varying, and (ii) the lumped variable can be, in principle, inferred from the conversion (and its derivative) experimental data, assuming that the k_p -behavior and the remaining parameters contained in K are known. From the application of the chain rule and simple algebraic manipulations one obtains:

$$x_1' = (1 - x) N_{1K}, \quad x(0) = x_0 \quad (3a)$$

$$\dot{x}_m = (1 - x_m) \left(\rho_m N_m - \frac{k_m N_{1K}}{\alpha k_p} \right); \quad (3b)$$

$$x_m(0) = 0$$

$$\dot{N}_{1K} = \alpha k_p \rho_m N_{m0} (1 - x_m) - k N_{1K} + \frac{N_{1K}}{k_p} \kappa; \quad N_{1K}(0) = 0 \quad (3c)$$

Equation set 3a-c is equivalent to set 1a-c after the change of variable mentioned above, where N_{1K} ($=N_1 K$) is the previously stated lumped parameter, $x_m = (N_{mo} - N_m) / N_{mo}$, $\alpha = K/k_p$, and κ represents the time variation of k_p that can be obtained assuming any copolymerization model (e.g. Ultimate, Penultimate or Bootstrap).^[13] The parameters to be estimated are: the entry to micelles ρ_m (s^{-1}), the exit rate from particles k (s^{-1}) and the rate coefficients of surfactant transport from micelles to particles k_m ($L s^{-1}$). Also the initial number of micelles is unknown. Here, the Ultimate model^[13] is adopted for simplicity and the assumption that the monomer composition is the same in micelles and in particles is applied as a first approach to this pseudo-homogeneous copolymerization model.

Following the ID method,^[4–7] our modeling problem solution is as follows: (i) apply regression (integral method) to smooth the experimental conversion data and obtain its derivative, (ii) draw the corresponding active particle evolution $N_{1a}(t)$ (observability-based differential method), (iii) regard the inferred evolution $N_{1a}(t)$ as an additional measurement, assume a copolymerization model for k_p

and a reasonable initial micelles concentration (N_{mo}), and apply regression (integral method) to fit the three-parameter set ρ_m - k - k_m of the three-differential equation model (3) against the augmented measurement data $y(t) = N_{1a}(t)$, (iv) compare the results with the experimental data, verify the impact of assuming N_{mo} , and (v) ratify or rectify the hypotheses.

Results

The proposed model was applied to the styrene-acrylonitrile ME polymerization data reported previously by Sanghvi et al.,^[2] where the effects of initiator concentration, temperature and initial monomers mixture composition were studied. The parameters used in the model are listed in Table 1. In this table, the homopolymerization propagation rate constants for styrene (k_s) and acrylonitrile (k_{AN}) and the reactivity ratios (r_s and r_{AN}) required by the Ultimate model are listed.

Initiator Concentration Effects

The symbols in Figure 1 represent the inferred N_{1a} (Eq 1e) and the model predictions (N_{1K}) against time. It can be seen that the model describes qualitatively well the bell-shaped form of the curves, a result which is opposed to previous reports where a linear growth of active particles was assumed.^[2,10,12] However, the model under-predicts the inferred lumped variable. The bell-shaped form of the nucleation rate has been reported before in emulsion polymerization for

Table 1.
Model parameters.

Parameter	Value	Reference
C_m (mol L ⁻¹)	6.88	[2]
M_0 (mol L ⁻¹)	0.637	[2]
k_s (L mol ⁻¹ s ⁻¹)	$2.88 \times 10^7 \exp(-3789/T)$	[14]
k_{AN} (L mol ⁻¹ s ⁻¹)	$1.047 \times 10^8 \exp(-3663/T)$	[15]
r_s (-)	0.85	[2]
r_{AN} (-)	0.82	[2]

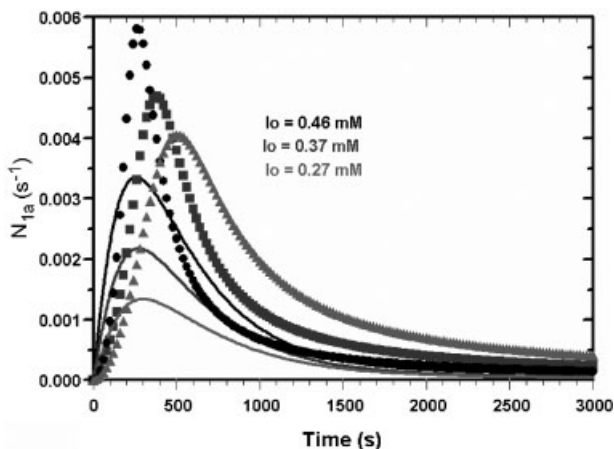


Figure 1.

Inferred lumped variable against reaction time from the differential (D) method step, for three initiator concentrations. Inferred variable (N_{1a}) data (symbols) and the model predictions (N_{1k}) from the integro-differential (ID) method results (continuous lines). The reaction temperature is 70 °C, initial STY-AN monomer composition ratio is 1-1, and the assumed initial micelles concentration is $1 \times 10^{22} \text{ L}^{-1}$.

the extended coagulative nucleation mechanism,^[16 and references therein] treated analyzing the particle size distribution.

Also, this bell-shaped form has been reported analyzing micellar against homogeneous nucleation^[17,18] assuming size dependent rate coefficients and distinct entry rates for ionic radicals, generated by the initiator, and non-ionic ones, produced by transfer-to-monomer reactions. The inferred lumped parameter maximum (Eq 1e) occurred at overall monomer conversions between 0.4 to 0.47. It has been claimed,^[19] assuming a linear radical growth, that the conversion at which the maximum rate occurs is 0.39.

Figure 2 shows that the model adequately describes the S-shaped form of the conversion curves, although the model predictions differ slightly from experimental data at low and intermediate conversions. These differences decrease with increasing initiator concentration. In this figure, it is clear that there is a small inhibition time which decreases as initiator concentration increases, which perhaps is the reason the model does not describe the conversion evolution exactly.

Table 2 presents the estimated parameters values as well as their respective

statistical standard deviations. There is an increase in radical entry rate to micelles as the concentration of initiator increases because the rate of generation of radicals increases, which also causes faster reactions and an increase in the number of active particles (Figure 1).

Since k (as well as the other parameters) is assumed to have a constant value, its variation (as well as the others) is within the standard deviations. The parameter k_m , in turn, decreases as initiator concentration is increased which may be due to a higher surfactant competition from the growing particles – the higher the initiator concentration, the higher number of active particles – therefore, less surfactant can be distributed from the micelles.

Because the initial number of micelles is unknown, the effect of this assumption on the estimated parameters is evaluated. Table 3 shows that the only parameter that is affected by varying the initial amount of micelles, is the entry to micelles coefficient, as expected.

Temperature Effects

Figure 3 depicts the inferred lumped variable behavior of model predictions (continuous lines) and the inferred variable

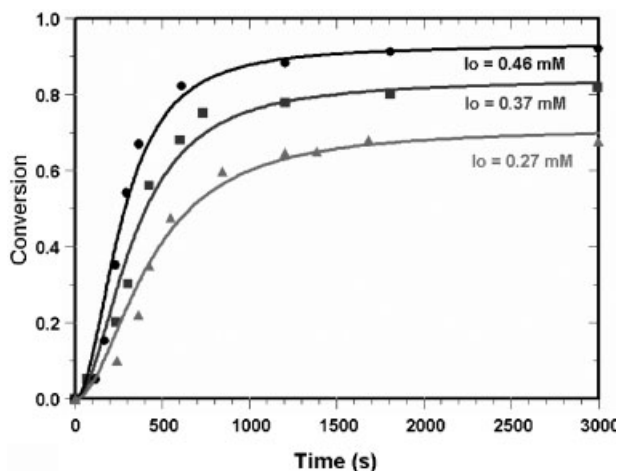


Figure 2.

Conversion against reaction time for three initiator concentrations: Experimental data (symbols), and the ID method-based model predictions (continuous lines). The reaction temperature is 70 °C, initial STY-AN monomer ratio is 1:1, and the assumed initial micelles concentration is $1 \times 10^{21} \text{ (L}^{-1}\text{)}$.

(symbols). Here, the under-prediction occurs only at the lower temperatures; however, the model also satisfactorily depicts the bell-shaped form. These results confirm again that there is no linear growth of active particles throughout the reaction, as it has been assumed elsewhere.^[2,10,12] Here, the inferred active particles' maximum (Eq 1e) occurs between 0.25 and 0.5 conversion, depending on the reaction temperature.

Figure 4 discloses that the model describes the S-shaped form of the conversion curves. Some differences in the model predictions with experimental data are evident at low and intermediate temperatures.

In this figure inhibition can also be detected at the intermediate and lowest

temperatures, which possibly explains why the model does not describe the conversion evolution as well as it does for the highest temperature.

Table 4 presents the estimated parameters values, as well as their respective statistical standard deviation reports. As expected, ρ_m increases greatly as temperature increases, because the initiator decomposes faster giving as a result a larger number of active particles (Figure 3) and faster reaction rates (Figure 4).

The desorption constant k increases with temperature, which can be explained by the larger mobility of the radical formed by chain transfer to monomer, which in turn increases the possibility for radicals' exit.

Table 2.

Effect of initiator content. Reaction temperature 70 °C, $N_{mo} = 1 \times 10^{21} \text{ L}^{-1}$, and initial STY-AN ratio:1:1

$l_0 \text{ (mM)} \rightarrow$ Parameters \downarrow	0.27	0.37	0.46
$k \text{ (s}^{-1}\text{)}$	2.355×10^{-3}	2.64×10^{-3}	2.98×10^{-3}
std. dev.	5.03×10^{-4}	4.56×10^{-4}	5.12×10^{-4}
$\rho_m \text{ (s}^{-1}\text{)}$	6.44×10^{-7}	1.16×10^{-6}	1.89×10^{-6}
std. dev.	1.76×10^{-8}	2.84×10^{-8}	5.07×10^{-8}
$km \text{ (L s}^{-1}\text{)}$	6.14×10^{-20}	4.12×10^{-20}	2.67×10^{-20}
std. dev.	1.37×10^{-20}	7.14×10^{-21}	4.26×10^{-21}

Table 3.

Effect of initial micelle concentration. Reaction temperature 70 °C, $l_0 = 0.37 \text{ mM}$, and initial STY-AN ratio:1:1

$N_{mo} \text{ (L}^{-1}\text{)} \rightarrow$ Parameters \downarrow	1×10^{20}	1×10^{21}	1×10^{22}
$k \text{ (s}^{-1}\text{)}$	2.64×10^{-3}	2.64×10^{-3}	2.64×10^{-3}
std. dev.	4.6×10^{-4}	4.56×10^{-4}	4.54×10^{-4}
$\rho_m \text{ (s}^{-1}\text{)}$	1.15×10^{-5}	1.16×10^{-6}	1.15×10^{-7}
std. dev.	2.84×10^{-8}	2.84×10^{-8}	2.84×10^{-9}
$km \text{ (L s}^{-1}\text{)}$	4.11×10^{-20}	4.12×10^{-20}	4.12×10^{-20}
std. dev.	7.18×10^{-20}	7.14×10^{-21}	7.08×10^{-21}

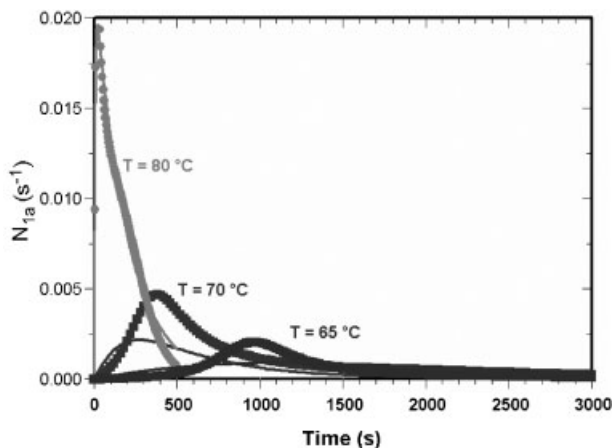


Figure 3.

Inferred lumped variable against reaction time for three temperatures: Inferred variable (N_{1a}) data from D method step (symbols), and the model predictions (N_{1k}) from the ID method result (continuous lines). The initiator concentration is 0.37 mM, initial STY-AN monomer ratio is 1-1, and the assumed initial micelles concentration is $1 \times 10^{22} \text{ L}^{-1}$.

Initial Monomer Composition Ratios

Effects

Figure 5 shows that the reaction rate increases as the monomer mixture becomes richer in styrene. This is the result of the larger styrene local concentration within the reacting particles and the faster styrene reactivity.

Once more the model adequately represents the bell-shaped form, but again it under-estimates the inferred lumped variable. In this case, the inferred active particles' maximum (Eq 1e) occurs between 0.35 and 0.5 conversion depending on the initial monomer ratio. Figure 6 reports conversion versus time as a function

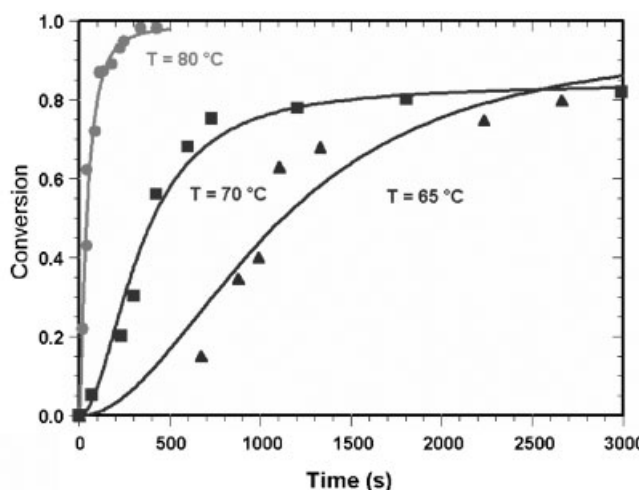


Figure 4.

Conversion against reaction time for three temperatures: Experimental data (symbols), and the model predictions ID method result (continuous lines). The initiator concentration is 0.37 mM, initial STY-AN monomer ratio is 1-1 and the assumed initial micelles concentration is $1 \times 10^{21} \text{ L}^{-1}$.

Table 4.

Effect of temperature. $I_0 = 0.37 \text{ mM}$, $N_{m0} = 1 \times 10^{21} \text{ (L}^{-1}\text{)}$, and initial STY-AN:1-1

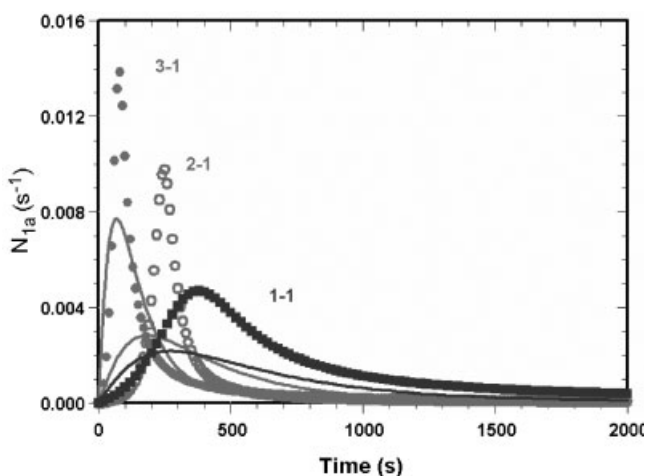
T (°C) → Parameters ↓	65	70	80
$k \text{ (s}^{-1}\text{)}$	7.45×10^{-4}	2.64×10^{-3}	5.21×10^{-3}
std. dev.	3.17×10^{-3}	4.56×10^{-4}	5.19×10^{-5}
$\rho_m \text{ (s}^{-1}\text{)}$	1.35×10^{-7}	1.16×10^{-6}	1.24×10^{-4}
std. dev.	4.64×10^{-8}	2.84×10^{-8}	2.31×10^{-5}
$k_m \text{ (L s}^{-1}\text{)}$	1.81×10^{-20}	4.12×10^{-20}	2.33×10^{-19}
std. dev.	7.72×10^{-20}	7.14×10^{-21}	5.77×10^{-21}

of initial monomer composition ratio. The model describes satisfactorily the S-shaped form but at low and intermediate conversions there are slight differences between the model and the experimental data; Figure 6 also reveals that inhibition occurs.

Table 5 shows that ρ_m and k increase as the STY-AN ratio increases. The increase in ρ_m can be explained by the larger affinity of STY with the organic phase which facilitates the radicals entrance to micelles, when the aqueous phase has more STY. The desorption constant increases at higher STY ratio, because the chain monomer transfer (C_M)^[13] of STY (0.6×10^{-4}) is larger than that of AN (0.3×10^{-4}), causing the probability for radical exiting to be larger since more monomeric radicals are formed inside the particles.

Conclusions

The problem of modeling and assessment in microemulsion copolymerization was studied by applying the ID method.^[4–7] The differential estimation consideration allowed calculating the active particles' time evolution, whose dependence was not linear with time, as opposed to the linear evolution hypothesis suggested in other works. This active particles' functional dependence was used as an inferred measurement, which contained additional information and permitted the estimation, with rather good error report, of three parameters (ρ_m , k , k_m) that could not have been obtained with the integral method alone. The maximum at which the inferred active particles occurred ranged from 0.25 to 0.5, conversion, which is within the reported value of 0.39 reached under different assumptions and for microemulsion homopolymerization. This approach does not require relying on a constant number of particles, as demanded by the slope-and-intercept method, to estimate entry and exit rate coefficients. In many cases, the model under-predicted the inferred lumped parameter containing the active particles evolution. One possible

**Figure 5.**

Inferred lumped variable (symbols), and model prediction from the ID method result (continuous lines) against reaction time for three initial monomer composition ratios of ST-AN. The initiator concentration is 0.37 mM, and the assumed initial micelles concentration is $1 \times 10^{22} \text{ L}^{-1}$.

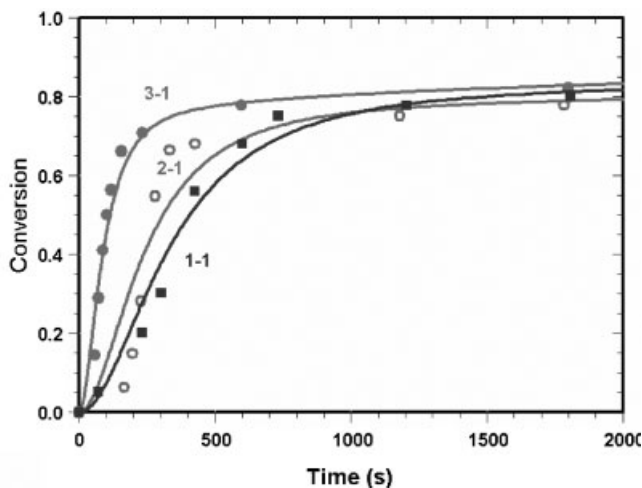


Figure 6.

Conversion against reaction time for three S-AN initial monomer ratios: Experimental data (symbols) and model predictions from the ID method result (continuous lines). The initiator concentration is 0.37 mM, temperature is 70 °C and the assumed initial micelles concentration is $1 \times 10^{21} \text{ L}^{-1}$.

cause of this miss-match is the omission of important mechanisms, such as competition of entry to particles, which was neglected *a priori* in the proposed model, based on previous results,^[4,5] and that will be revised in a future work. Concerning the homogeneous nucleation mechanism, also not considered, it is not expected to have a great impact,^[13] specially in the case of high tensoactive content as required in ME polymerization. Also, inhibition effects were evident in the experimental data that should be eliminated by performing replicate runs. In spite of these obstacles, the variation trends of ρ_m and k and k_m as a function of initiator concentration, temperature and monomers ratio were as expected. These results indicate that this

simplified model is capable of predicting overall conversion and determining this parameter parameter triplet with acceptable certainty. In a further step the model uncertainty can be formally established quantitatively by applying the stochastic error characterization technique^[7] of the ID model assessment method.

Acknowledgements: Funds for this work were provided by UNAM (PAPIIT IN103109-3 and PAIP 529030) and the interchange program between U de G and UNAM, and are gratefully acknowledged.

Table 5.

Effect of initial monomer S-AN composition ratios. Temperature 70 °C. $Io = 0.37 \text{ mM}$, $N_{mo} = 1 \times 10^{21} \text{ L}^{-1}$

STY-AN → Parameters ↓	3-1	2-1	1-1
$k \text{ (s}^{-1}\text{)}$	11.30×10^{-3}	3.90×10^{-3}	2.64×10^{-3}
std. dev.	3.3×10^{-4}	1.11×10^{-3}	4.56×10^{-4}
$\rho_m \text{ (s}^{-1}\text{)}$	2.24×10^{-5}	2.74×10^{-6}	1.16×10^{-6}
std. dev.	4.77×10^{-7}	1.19×10^{-7}	2.84×10^{-8}
$k_m \text{ (L s}^{-1}\text{)}$	3.12×10^{-20}	3.65×10^{-20}	4.12×10^{-20}
std. dev.	5.00×10^{-22}	1.02×10^{-20}	7.14×10^{-21}

- [1] B. Hawket, D. H. Napper, R. G. Gilbert, J. C. S. Faraday J **1980** 76, 1323.
- [2] P. G. Sanghvi, N. K. Pokhriyal, P. A. Hassan, S. Devi, Polym Int **2000**, 49, 1417.
- [3] V. M. Ovando-Medina, E. Mendizábal, R. D. Peralta, Pol Bull **2005**, 54, 129.
- [4] F. López-Serrano, J. E. López-Aguilar, E. Mendizábal, J. E. Puig, J. Álvarez, Macromol Symp **2008**, 271, 94.
- [5] F. López-Serrano, J. E. López-Aguilar, E. Mendizábal, J. E. Puig, J. Álvarez, Ind Eng Chem Res **2008**, 47, 5924.
- [6] F. López-Serrano, J. E. Puig, J. Álvarez, Ind. Eng. Chem. Res. **2004**, 43, 7361.
- [7] F. López-Serrano, J. E. Puig, J. Álvarez, Ind. Eng. Chem. Res. **2007**, 46, 2455.

- [8] J. Alvarez, *J. Process Control* **2000**, 10, 59.
- [9] A. L. Polic, L. M. F. Lona, T. A. Duever, A. Penlidis, *Macromol. Theory Simul.* **2004**, 13, 115.
- [10] C. C. Co, R. de Vries, E. W. Kaler, *Macromolecules* **2001**, 34, 3224.
- [11] W. R. Esposito, C. A. Floudas, *Ind. Eng. Chem. Res.* **2000**, 39, 1291.
- [12] M. Nomura, K. Suzuki, *Ind Eng Chem Res* **2005**, 44, 2561.
- [13] G. Odian, “*Principles of Polymerization*”, 4th Ed., Wiley, New York 2004.
- [14] S. Beuermann, M. Buback, *Prog Polym Sci* **2002**, 27, 191.
- [15] A. Keramopoulos, C. Kiparissides, *Macromolecules* **2002**, 35, 4155.
- [16] E. Gianneti, *AIChE J* **1993**, 39(7), 1210.
- [17] J. Herrera-Ordóñez, R. Olayo, *J. Polym A Pol Chem* **2000**, 48, 2201.
- [18] J. Herrera-Ordóñez, R. Olayo, *J. Polym A Pol Chem* **2000**, 48, 2219.
- [19] J. D. Morgan, K. M. Lusvardi, E. Kaler, *Macromolecules* **1997**, 30, 1897.